Secondary Microseisms generated by typhoons in the Northwestern Pacific Ocean

Nassima Benbelkacem[1], Eléonore Stutzmann[1], Martin Schimmel[2], Véronique Farra[1], Fabrice Ardhuin[3], Guilhem Barruol[1], and Anne Mangeney[1]

[1]Université de Paris, Institut de Physique du Globe de Paris, CNRS - [2]Institut of Earth Sciences Jaume Almera-CSIC, Barcelona, Spain - [3]Ifremer, Laboratoire d'Océanographie Physique et Spatiale, IUEM, Brest, France

INTRODUCTION

Secondary Microseisms (SM) are recorded by seismometers in the period band 3-10 s. They are generated by the interaction of ocean gravity waves of similar frequencies and coming from nearly opposite directions. According to Ardhuin et al. [2011] SM generation event can be clustered in three broad classes : wind waves with a broad directional spectrum (class I), sea states with a significant contribution of coastal reflections (class II), and the interaction of two independent wave systems (class III).

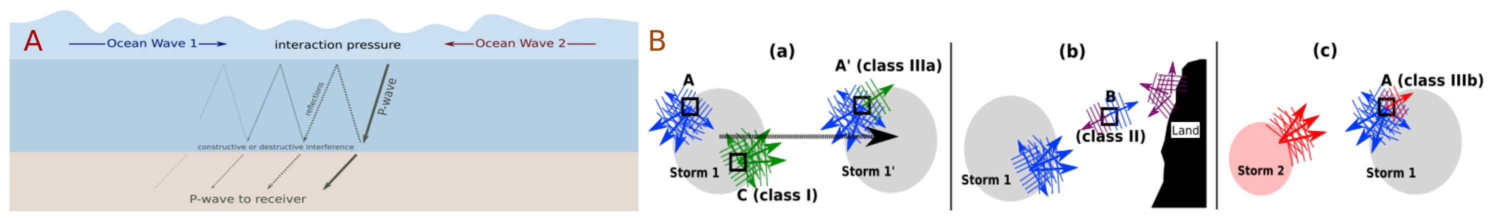

Figure 1 : A) Mechanism of SM generation (Meschede et al. [2017]). B) Schematic of wave conditions in noise-generating situations (Ardhuin et al. [2011]).

The goal of this work is to examine the relationship between typhoons and SM source characteristics in the Northwestern Pacific ocean. We compared the observed and the modelled beam PSD for Alaska array every 6 hours to retrieve SM sources generated by two typhoons, Lekima and Krosa acting simultaneously.

METHODOLOGICAL APPROACH

Real beam

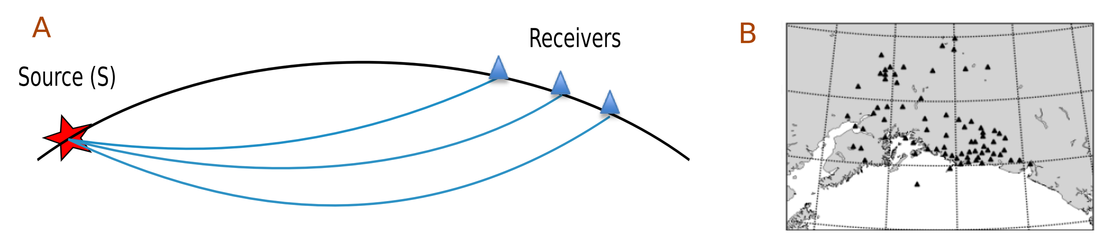

Figure 2 : A) Sketch of seismic wave propagation from the source to the receiver. B) Alaska array used in this study.

The power spectral density B(f,s) at frequency f and horizontal slowness ***s*** is given by:

$$B_{\mathrm{w}}(f,\mathbf{s}) = \frac{1}{N^2}\left|\sum_{j=1}^{N} S_j(f)e^{-i2\pi f\mathbf{s}\cdot(\mathbf{x}_j-\mathbf{x}_c)}\right|^2$$

Where $S_j(f)$ the Fourier spectra of the trace at station j., $\mathbf{x}_j$ and $\mathbf{x}_c$ are the positions of station j and the array center, respectively.

$w(f,\mathbf{s})$ is the weight factor which mesures the coherency of the incoming wavefield independently of its amplitude.

$$w(f,\mathbf{s}) = \frac{1}{N^2}\left|\sum_{j=1}^{N} \frac{S_j(f)}{|S_j(f)|}e^{-i2\pi f\mathbf{s}\cdot(\mathbf{x}_j-\mathbf{x}_c)}\right|^2.$$

The final phase-weighed beam PSD is :

$$B_{\mathrm{pw}}(f,\mathbf{s}) = w(f,\mathbf{s})B_{\mathrm{w}}(f,\mathbf{s}).$$

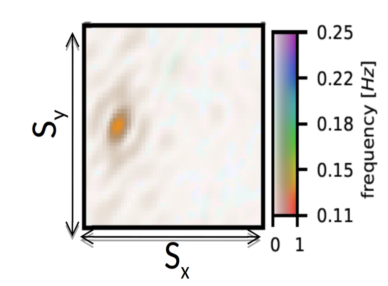

Meschede et al. [2017]

Synthetic beam

Farra et al. [2016] showed that the P-wave displacement in the far field can be computed in the frequency domain as the product of (1) the pressure sources (WAVEWATCHIII), (2) the source site effect (Guilteri et al. [2014]), (3) the propagation term from the ocean bottom to the seismic stations, and (4) the receiver site effect.

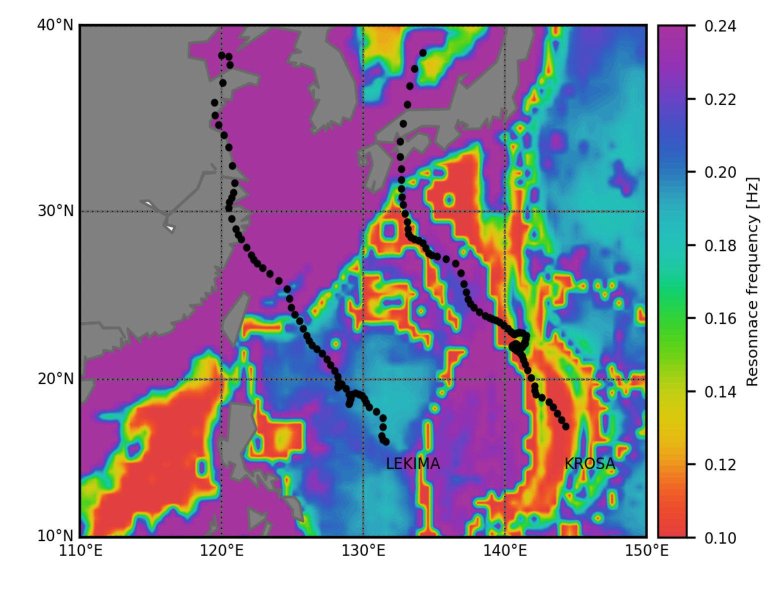

Figure 3 : Source site effect : Map of resonance frequencies within the frequency band (0.10-0.24 Hz) in the region of interest.

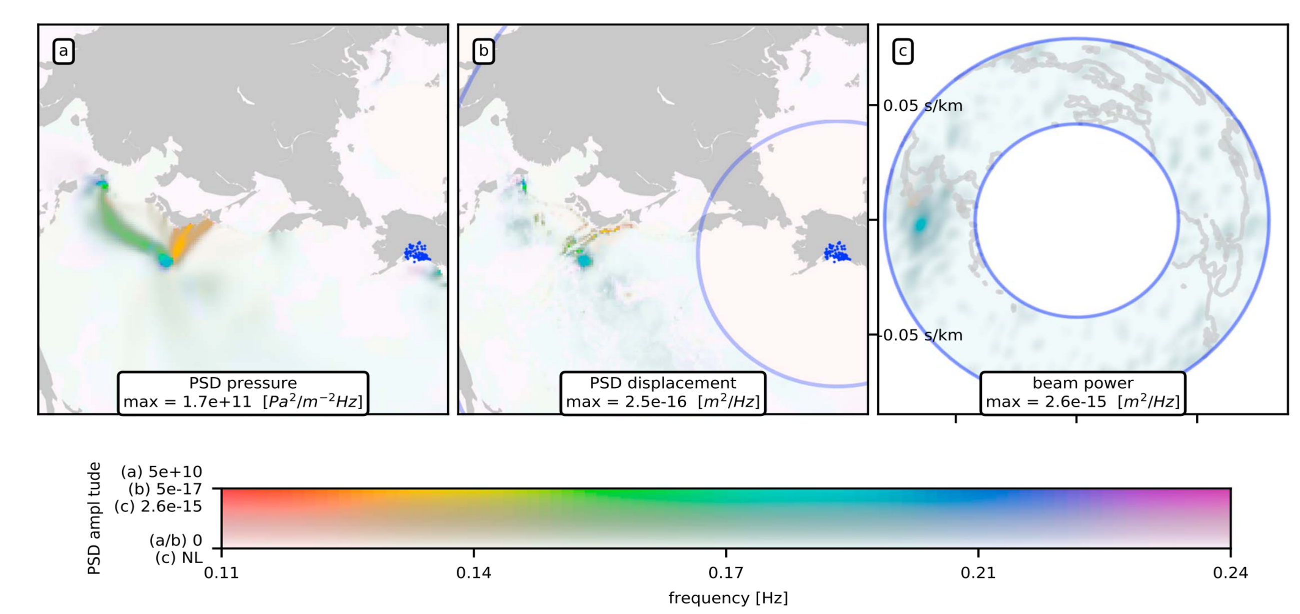

Figure 4 : Example of synthetic beam construction for the Alaska array on 23 August 2015. (a) Pressure PSD. (b) Displacement PSD. and c) Synthetic beam PSD (Meschede et al. [2017]).

RESULTS

Case 1
SM generated by wave interaction within Lekima typhoon (class I)

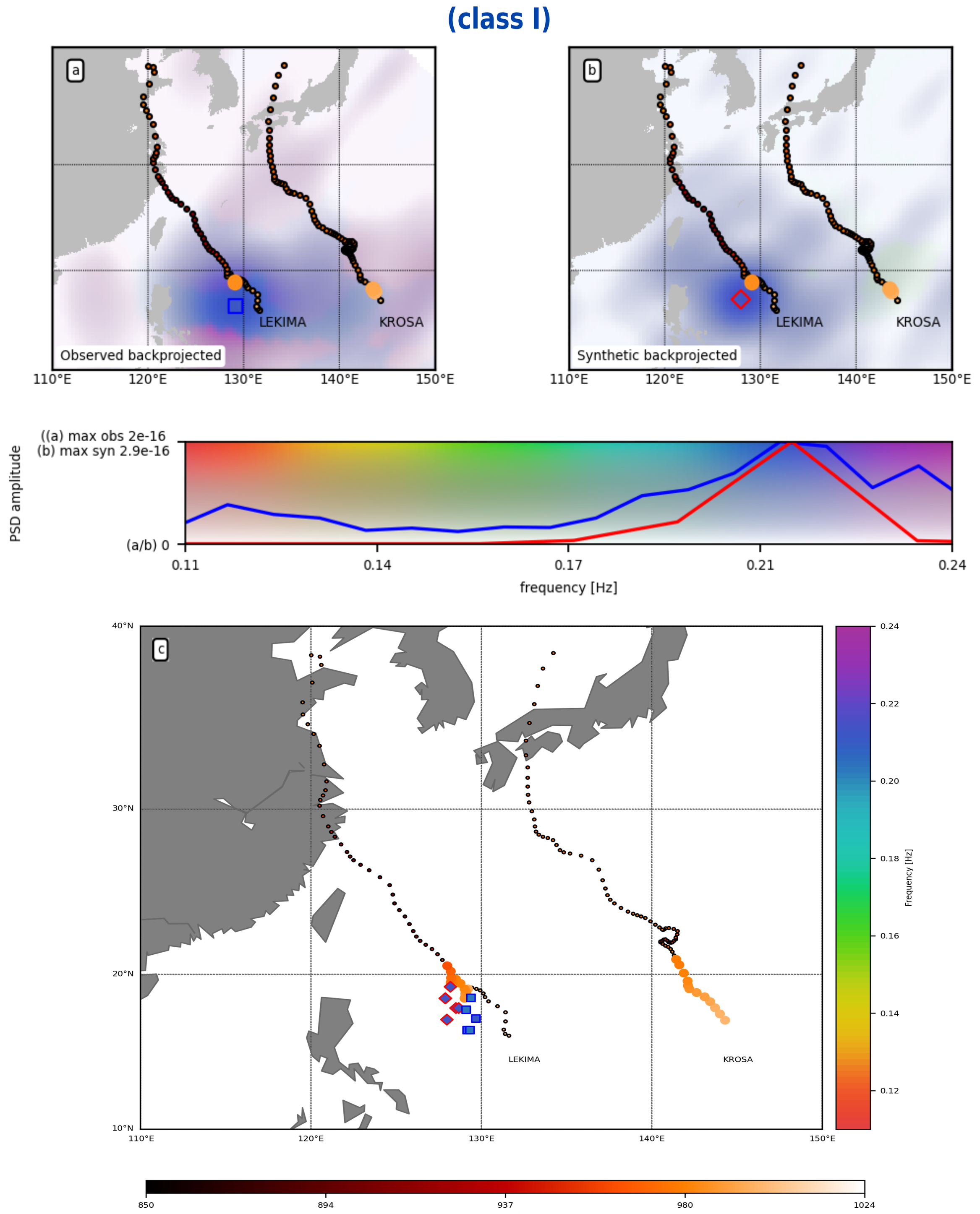

Case 2 :
SM generated by waves interaction between typhoon Lekima and typhoon Krosa (class III)

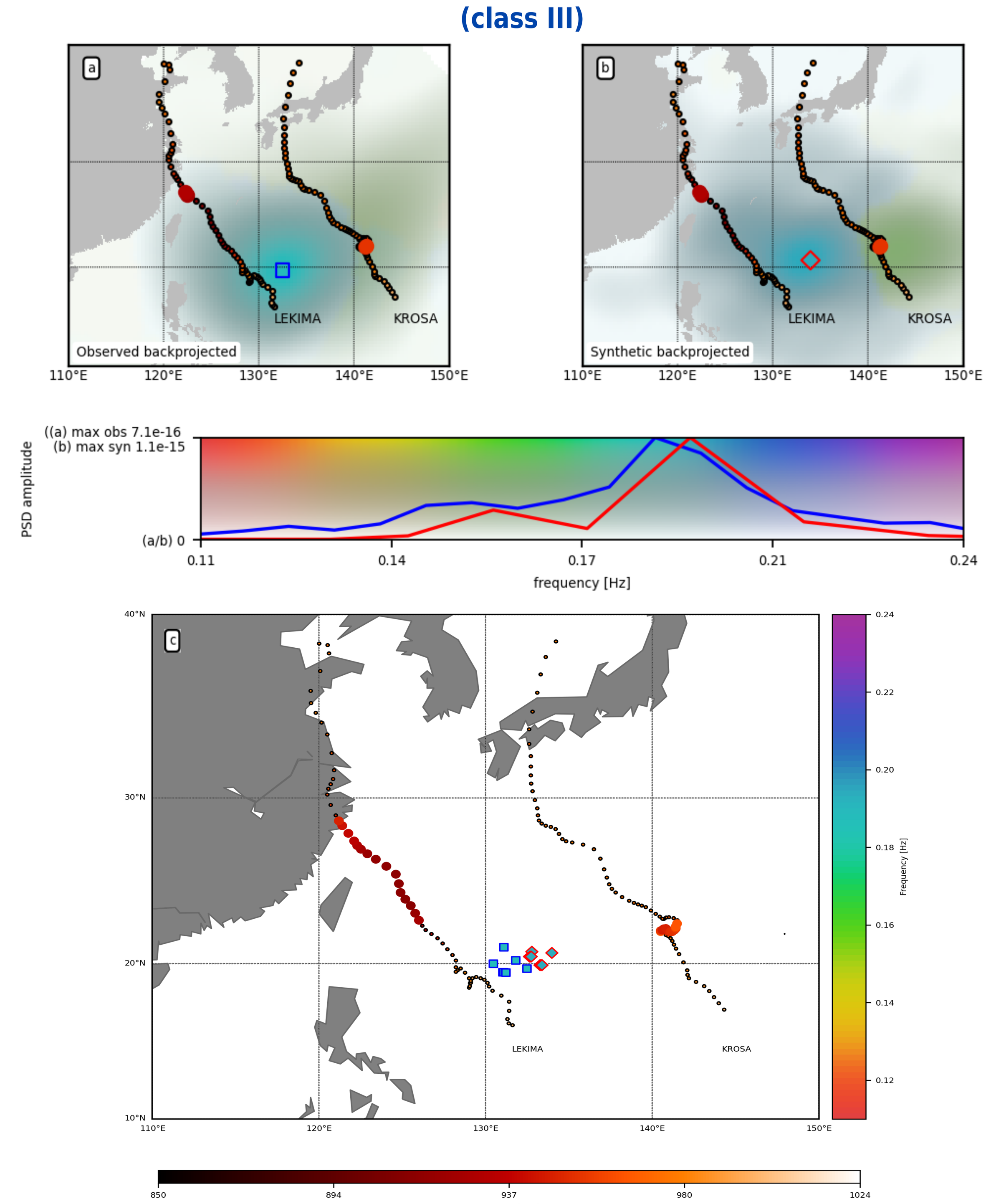

Case 3
SM generated by wave interaction within Krosa typhoon (class I)

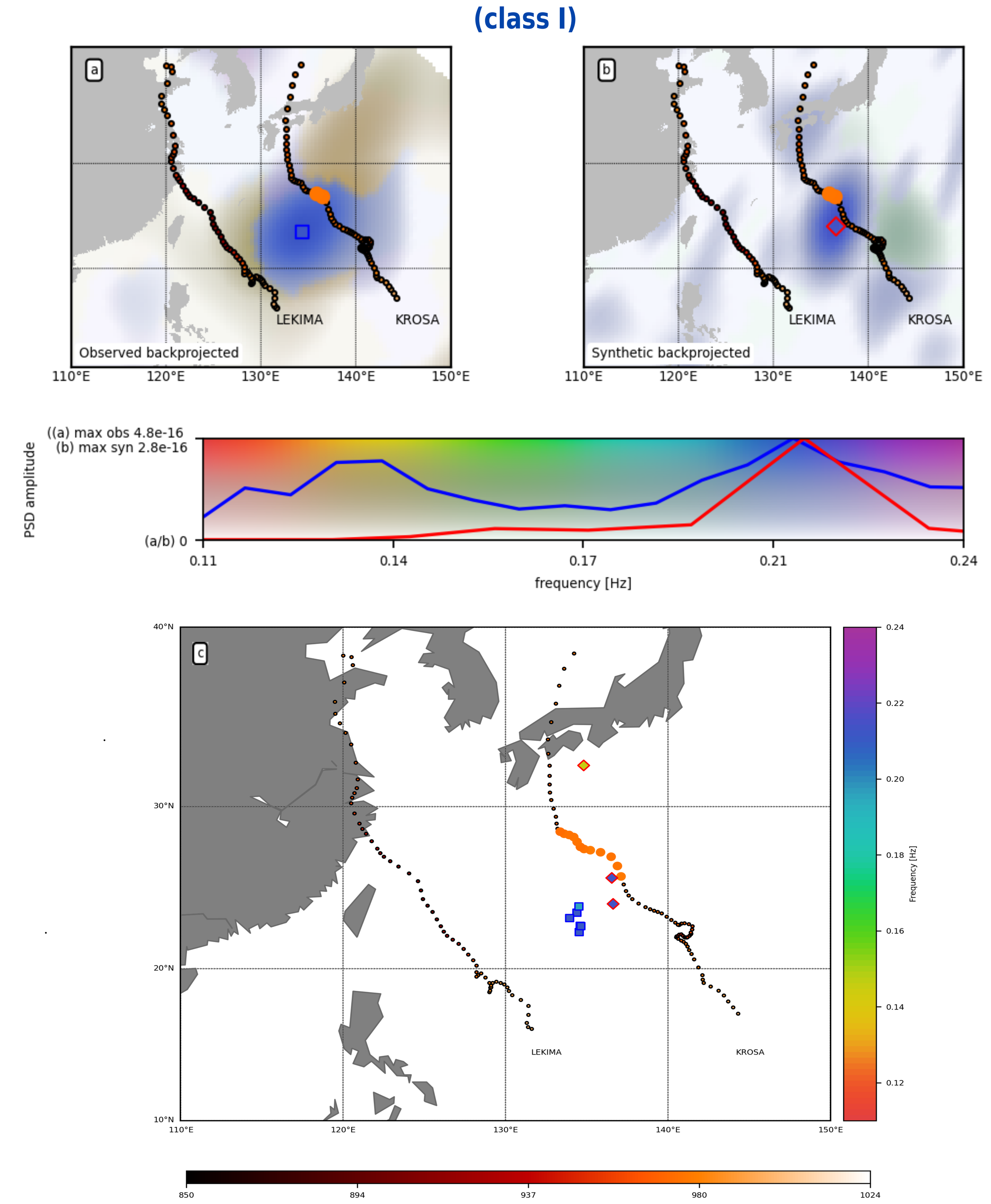

Figure 5 :Three different cases showing two classes of SM sources generation, in each case: a) Observed backprojected beam PSD and b) synthetic backprojected beam PSD at the Alaska array calculated over 6 hours. The dominate frequency and the corresponding beam PSD maximum are represented by the color hue and the color lightness respectively. The red and blue spectra in the color bar refer to the strongest source spectra from a and b that are indicated by the blue square and the red diamond respectively. c) Body waves seismic sources location (observed in square, and modelled in diamond) associated to the colored part of the typhoon Lekima or/and the typhoon Krosa.

- Typhoon path
- Active part of the Typhoon
- Max observed beam
- Max synthetic beam

CONCLUSIONS

* Beamforming technique applied to the vertical components of secondary microseismic noise allows to retrieve the amplitude and localisation of their sources generated by the typhoon Lekima and Krosa every 6 hours.

* This study shows two classes of secondary microseimic noise generation : class I due to one signal wind-sea (Typhoon Lekima or Krosa), and class III generated by two well separated storm acting simultaneously (Lakima and Krosa).

* Good correlation between observed and modelled secondary microseismic sources.

PERSPECTIVE

Source catalog → ***Differential traveltime measurements*** → ***Regional tomography***

References

- Ardhuin F., E. Stutzmann, M. Schimmel, A. Mangeney, 2011. The ocean wave sources of seismic noise, *J. Geophys. Res.*, 116, C09004, doi:10.1029/2011JC006952

- Farra V., E. Stutzmann, L. Gualtieri, M Schimmel, and F. Ardhuin, 2016. Ray-theoretical modeling of secondary microseism p waves.Geophysical Journal International,206(3) :1730–1739, doi: 10.1093/gji/ggw242.

- Gualtieri L., E. Stutzmann, V. Farra, Y. Capdeville, M Schimmel, F. Ardhuin, and A. Morelli, 2014. Modelling the ocean site effect on seismic noise body waves.Geophysical Journal International, 197(2) : 096–1106, doi: 10.1093/gji/ggu042.

- Longuet-Higgins, M, 1950. Theory of the origin of microseisms, Philos. Trans. R. Soc. A, 243, 1–35, doi:10.1098/rsta.1950.0012

- Meschede M., E. Stutzmann, V. Farra, M. Schimmel, F. Ardhuin, 2017. The effect of water column resonance on the spectra of secondary microseism P waves, *J. Geophys. Res.*, 122, 8121-8142., doi:10.1002/2017JB014014.